JOURNAL OF THERMOPHYSICS AND HEAT TRANSFER
Vol. 19, No. 3, July–September 2005

Design of Experiments for Thermal Characterization of Metallic Foam

Paul E. Crittenden*
Air Force Institute of Technology, Wright–Patterson Air Force Base, Ohio, 45433-7765
and
Kevin D. Cole†
University of Nebraska, Lincoln, Nebraska, 68588-0656

Metallic foams are being investigated for possible use in the thermal protection systems of reusable launch vehicles. As a result, the performance of these materials needs to be characterized over a wide range of temperatures and pressures. A radiation/conduction model is used to study heat transfer in metallic foams for the purpose of designing experiments to measure thermal properties. Candidates for the optimal transient experiment to determine the intrinsic thermal properties of the model are found by two methods. First, an optimality criterion is used in an experiment to find all of the parameters using one heating event. Second, a pair of heating events is used to determine the parameters in which one heating event is optimal for finding the parameters related to conduction, whereas the other heating event is optimal for finding the parameters associated with radiation. Simulated data containing random noise were analyzed to determine the parameters using both methods.

Nomenclature

a = coupling coefficient, $(\mathrm{m}\cdot\mathrm{K/W})^3$
b = heater thickness, m
b_k = normalized sensitivity coefficient for the kth parameter, units of F, a, ω, ϵ_0, and ϵ_1
c = foam specific heat, J/(kg · K)
c_g = specific heat of gas, J/(kg · K)
c_h = specific heat of heater, J/(kg · K)
c_m = specific heat of metal, J/(kg · K)
D = optimality criterion
D_f = fiber diameter, m
d_g = gas collision diameter, m
e = specific extinction coefficient, $e_0 + e_1 T$, m^2/kg
e_0 = temperature-independent part of e, m^2/kg
e_1 = linear variation of e with respect to T, $\mathrm{m}^2/(\mathrm{kg}\cdot\mathrm{K})$
F = efficiency factor for conduction
G = incident radiation, $\mathrm{W/m}^2$
G^i_j = incident radiation at the ith time step and jth node, $\mathrm{W/m}^2$
K_B = Boltzmann constant
Kn = Knudsen number
k = thermal conductivity, W/(m · K)
k_g = gas thermal conductivity, W/(m · K)
k^*_g = gas thermal conductivity at 1 atm, W/(m · K)
k_m = thermal conductivity of metal, W/(m · K)
L = sample thickness, m
ℓ = pore size of metallic foam, m
n = number of sample temperatures
P = pressure, mm Hg
Pr = Prandtl number
p = number of parameters
q_c = conduction heat flux, $\mathrm{W/m}^2$
q_{in} = heat flux into heater, $\mathrm{W/m}^2$
q_{out} = heat flux out of heater, $\mathrm{W/m}^2$
q^c_{out} = conduction heat flux out of heater, $\mathrm{W/m}^2$
q_r = radiation heat flux, $\mathrm{W/m}^2$
q^r_{out} = radiation heat flux out of heater, $\mathrm{W/m}^2$
q_T = total heat flux, $\mathrm{W/m}^2$
T = temperature, K
$\boldsymbol{T}$ = temporal temperature vector, K
T_c = cold plate temperature, K
T_h = heater temperature, K
T^i_j = temperature at the ith time step and jth node, K
T_{est} = estimated temperature, K
T_{exact} = exact temperature, K
T_{pert} = perturbed temperature, K
T_s = temperature at heated surface, K
T_0 = mirror temperature, K
t = time, s
$\boldsymbol{X}$ = sensitivity matrix, K^2
X_k = sensitivity coefficients, K
x = spatial coordinate, m
Z = gas conductivity adjustment
α = thermal accommodation coefficient
β = extinction coefficient, 1/m
γ = specific heat ratio
δ = perturbation value, Eq. (31)
ϵ = porosity
ϵ_h = emittance of mirror
ϵ_1 = emittance of the sample surface
ϵ_2 = emittance of cold plate
ζ = temperature-dependent material property function, varies
ζ_i = material property at ith node, varies
λ = gas molecular mean free path, m
ρ = density of foam, $\mathrm{kg/m}^3$
ρ_g = density of gas, $\mathrm{kg/m}^3$
ρ_h = density of heater, $\mathrm{kg/m}^3$
ρ_m = density of metal, $\mathrm{kg/m}^3$
σ = Stefan–Boltzmann constant
Φ = high-pressure indicator
Ψ = low-pressure indicator
ω = albedo of scattering

Received 26 November 2003; presented as Paper 2004-2170 at the AIAA 37th Thermophysics Conference, Portland, OR, 28 June–1 July 2004; revision received 25 October 2004; accepted for publication 30 October 2004.

*Visiting Assistant Professor, Department of Mathematics.
†Associate Professor, Mechanical Engineering Department. Member AIAA.

I. Introduction

HIGH-POROSITY metallic foams are being studied as possible components of aerospace thermal protection systems. The performance of these systems needs to be characterized over a wide range of temperatures and pressures during ascent and reentry.[1] In the future, when such materials are specified as part of a vehicle program, part of the procurement process will involve certification that the material meets the specifications.

To date there has been little research on experimental design for thermal characterization of high-porosity materials. The present research is intended to close this gap in the procurement cycle by investigating transient methods for accurate measurement of thermal properties in metal-foam materials. In this paper, only numerical simulations are presented.

A review of the pertinent literature is given next in the areas of optimal experimental design and heat transfer in high-porosity materials. Transient experiments combined with parameter estimation have been used for obtaining thermal properties for many years.[2] In these methods, the desired parameters are found by nonlinear regression between the experimental data (temperatures in this case) and a computational model of the experiment. Parameter estimation concepts have been applied to optimal experiment design for thermal characterization of uniform materials[3] and for materials with temperature-varying properties.[4] One of the authors has previously studied optimal experimental design for the measurement of thermal conductivity in low-conductivity materials[5] and in layered materials.[6] The work was limited to a small rise in temperature so that radiation heat transfer was negligible. An optimality criterion was used to find the best experimental conditions for the estimation of thermal properties.

There have been many studies of glass-fiber insulation, in which combined radiation and conduction heat transfer are present. Yuen et al.[7] used a detailed radiation model and measured optical properties to simulate the temperature response of a fibrous insulation material from first principles. The model involves a detailed determination of wavelength-dependent radiation exchange between multiple zones through the thickness of the material. Their results compared favorably to transient experimental tests carried out in 1974 on LI9000 sintered silica insulation (rigid space shuttle tile).

Insulation models based on optical properties, although science-based, do not provide direct evidence of the insulation's ability to withstand reentry heating. Simplified insulation models, combined with direct tests, can provide compelling evidence that a thermal protection system is ready for use on a human-piloted vehicle. Daryabeigi[8] used steady experiments to characterize low-density fibrous insulation over a wide temperature and pressure range, and a transient experiment was used to simulate reentry aerodynamic heating conditions. A combined radiation/conduction model was used, with the radiation described by a two-flux method assuming anisotropic scattering and a gray medium. Two models were discussed for combining solid and gas conduction into an effective conductivity, a parallel model, and a model based on fiber orientation. Thermal properties estimated with both models yielded similar results, and so it was not possible to choose one conduction model over the other. Low Rayleigh numbers and experimental verification ruled out free-convection heat transfer in the pores.

There have been several recent conduction-only studies of high-porosity metal foams. Boomsma and Poulikakos[9] predicted the effective thermal conductivity from models based on the morphology of the metal foam. Bhattacharya et al.[10] found agreement for the effective thermal conductivity between a morphological model and an empirical model with experimentally determined coefficients. In their empirical model, the effective conductivity is a combination of parrallel and series arrangements of heat conduction through the metal struts and the fluid-filled cells. In the present paper, we also use an empirical model to describe the conduction portion of the heat transfer.

There are few studies of open-cell metallic foams that include both radiation and conduction. Zhu et al.[11] carried out simulations of a titanium foam material for the purpose of finding the minimum weight of the thermal protection by varying the pore size of the foam across its thickness. Their steady-state model included effective conductivity and radiation parameters. Compared to uniform materials, a density-graded material provides the same protection with less weight, with greater percentage savings for thinner insulation. Sullins and Daryabeigi[12] studied a nickel-foam material over a wide range of temperatures and pressures with steady-state experiments combined with parameter estimation methods. The model for the heat transfer included a two-flux model for the radiation and combined gas/solid conduction. The effective conductivity was described by parallel gas/solid conduction, temperature-dependent gas conduction, and an efficiency factor for solid conductivity (as a small fraction of the bulk metal conductivity). A gas/solid coupling term was also added to take into account an observed increase in conductivity at higher pressures and temperatures. The measurement of the model parameters was carried out with a nonlinear regression technique applied to steady-state experiments, and the parameters were reported.

In this paper, the methods of optimal experimental design are applied to a high-porosity nickel-foam material, with thermal property values taken from Sullins and Daryabeigi.[12] Both conduction and radiation heat transfer are included. Based on a one-dimensional model of transient heat transfer, a large number of simulated experiments have been studied to determine which experimental conditions provide the best estimates of the thermal properties. No laboratory experiments are reported.

The paper is divided into several sections, as follows: analytical model, numerical solution, simulated experiments, optimality criterion, optimal experimental design, estimation of parameters, and conclusions.

II. Analytical Model

In this section, the heat transfer model of Sullins and Daryabeigi[12] and Daryabeigi[13] is used to model metallic foams. It is a one-dimensional, two-flux model taking into account both conduction and radiation heat transfer. Contained within the model are five parameters considered to be intrinsic properties of the material that must be determined empirically. Three of these intrinsic properties are related to the radiative heat transfer and two are related to heat transfer by conduction.

The transient heat equation with radiation is given by

$$\rho c \frac{\partial T}{\partial t} = -\frac{\partial q_c}{\partial x} - \frac{\partial q_r}{\partial x} \tag{1}$$

The conduction heat flux is given by

$$q_c = -k \frac{\partial T}{\partial x} \tag{2}$$

The gradient of the radiant heat flux is given by

$$\frac{\partial q_r}{\partial x} = \beta(1-\omega)(4\sigma T^4 - G) \tag{3}$$

The albedo of scattering ω is to be determined experimentally. The incident radiation is related to the radiant heat flux by

$$q_r = -\frac{1}{3\beta}\frac{\partial G}{\partial x} \tag{4}$$

Thus, Eq. (1) becomes

$$\rho c \frac{\partial T}{\partial t} = \frac{\partial}{\partial x}\left(k \frac{\partial T}{\partial x}\right) + \frac{1}{3\beta}\frac{\partial^2 G}{\partial x^2} \tag{5}$$

The incident radiation G satisfies the second-order differential equation

$$\frac{1}{3\beta^2(1-\omega)}\frac{\partial^2 G}{\partial x^2} + G = 4\sigma T^4 \tag{6}$$

on the interior. On the boundary, G must satisfy

$$-\frac{2}{3\beta[\epsilon_1/(2-\epsilon_1)]}\frac{\partial G}{\partial x}+G=4\sigma T_s^4, \qquad x=0 \tag{7}$$

$$\frac{2}{3\beta[\epsilon_2/(2-\epsilon_2)]}\frac{\partial G}{\partial x}+G=4\sigma T_c^4, \qquad x=L \tag{8}$$

where T_s is the temperature of the surface of the sample, T_c is the temperature of the cold plate (300.6 K), $\epsilon_1=0.85$ is the emittance of the surface, and $\epsilon_2=0.92$ is the emittance of the cold plate.

Next, the material properties will be discussed for a specific high-porosity nickel foam in an N_2 atmosphere. The product ρc for the foam is the weighted average of the values for the metal (nickel) and the gas (nitrogen). Explicitly,

$$\rho c=\rho_m c_m(1-\epsilon)+\rho_g c_g \epsilon \tag{9}$$

The density ρ_g and specific heat c_g of the gas are temperature dependent and given in the Appendix. For nickel,[14] ρ_m is taken to be 8900 kg/m^3 and $c_m=444.0$ J/(kg $\cdot$ K). The porosity ϵ is 0.968 for nickel foam.

Heat conduction is assumed to occur in parallel in the gas and solid with some coupling in the form

$$k=\epsilon k_g+(1-\epsilon)Fk_m+a(Fk_g k_m)^2 \tag{10}$$

The thermal conductivity of the metal is a function of temperature and is interpolated from tabulated data.[15] For the gas

$$k_g=k_g^*\big/Z \tag{11}$$

where k_g^* is the temperature dependent conductivity of the gas at atmospheric pressure (see the Appendix) and Z is given by

$$Z=\Phi+4\Psi\frac{(2-\alpha)\gamma Kn}{\alpha(\gamma+1)Pr} \tag{12}$$

In this expression, the thermal accommodation coefficient α is taken to be one, $\gamma=1.4$ is the specific heat ratio, and Pr is the temperature-dependent Prandtl number (see Appendix). The Knudsen number is given by

$$Kn=\lambda/\ell \tag{13}$$

The quantities Φ and Ψ were defined[12] as

$$\Phi=\begin{cases}1, & Kn<10\\ 0, & Kn>10\end{cases} \tag{14}$$

$$\Psi=\begin{cases}0, & Kn<0.01\\ 1, & Kn>0.01\end{cases} \tag{15}$$

This was to provide an approximation of Z in the different ranges by neglecting one term when it was much smaller than the other. However, determining the optimum experiment requires finding the derivative of the temperature at the sensor with respect to the empirical parameters. Having a discontinuous expression for the gas conductivity resulted in inaccurate results for these derivatives when the simulated experiments were done near the boundary between two of the ranges for Kn. Therefore, in this work, $\Phi=\Psi\equiv 1$.

The pore size for the metallic foam was assumed to be in the same form as that given by Daryabeigi[13] and is given by

$$\ell=(\pi/4)[D_f/(1-\epsilon)] \tag{16}$$

In this expression $D_f=1.4E-5$ m is the diameter of the strut. The mean free path is given by

$$\lambda=\frac{K_B T}{\sqrt{2}\pi P d_g^2} \tag{17}$$

in which $K_B=1.38E-23$ is the Boltzmann constant and $d_g=3.798E-10$ m is the gas collision diameter.

The extinction coefficient is given by

$$\beta=e\rho \tag{18}$$

The specific extinction coefficient is taken to be a linear function of the temperature. Explicitly,

$$e=e_0+e_1 T \tag{19}$$

The quantities e_0, and e_1 are considered to be intrinsic properties of the media to be determined experimentally.

Thus, for this model, heat transfer in a metallic foam is determined by the intrinsic properties F, a, e_0, e_1, and ω. The goal is to find the optimal transient experiment to determine these parameters. The variables considered for different experiments are the heating power, sensor location, heating time, and pressure.

III. Numerical Solution

The heat equation (5) and the radiation equation (6) are solved numerically. For each time step of the heat equation, the radiation equation is discretized and solved. The solution is then used in a discretized form of the heat equation to determine the temperatures for the next time step. The temperatures are then replaced with the new temperatures, and the process is repeated.

Discretizing Eqs. (6–8) gives the tridiagonal system of equations

$$\begin{bmatrix}B_1 & C_1 & 0 & 0 & 0 & \dots & 0\\ A_2 & B_2 & C_2 & 0 & 0 & \dots & 0\\ 0 & A_3 & B_3 & C_3 & 0 & \dots & 0\\ 0 & 0 & \ddots & \ddots & \ddots & \ddots & 0\\ 0 & 0 & 0 & \ddots & \ddots & \ddots & 0\\ 0 & 0 & 0 & \dots & A_{N-1} & B_{N-1} & C_{N-1}\\ 0 & 0 & 0 & \dots & 0 & A_N & B_N\end{bmatrix}\begin{bmatrix}G_1\\ G_2\\ \vdots\\ \vdots\\ \vdots\\ \vdots\\ G_N\end{bmatrix}$$

$$=\begin{bmatrix}4\sigma(T_1)^4\\ 4\sigma(T_2)^4\\ \vdots\\ \vdots\\ \vdots\\ \vdots\\ 4\sigma(T_N)^4\end{bmatrix} \tag{20}$$

where G_i and T_i are the radiation and temperature, respectively, at node i. The elements of the coefficient matrix are given by

$$A_i=\begin{cases}-\dfrac{2}{3\beta_i^2(1-\omega)\Delta x_{i-1}(\Delta x_{i-1}+\Delta x_i)}, & i=2,\dots,N-1\\ -\dfrac{2(2-\epsilon_2)}{3\beta_i\epsilon_2\Delta x_{i-1}}, & i=N\end{cases} \tag{21}$$

$$C_i=\begin{cases}-\dfrac{2(2-\epsilon_1)}{3\beta\epsilon_1\Delta x_i}, & i=1\\ -\dfrac{2}{3\beta_i^2(1-\omega)\Delta x_i(\Delta x_{i-1}+\Delta x_i)}, & i=2,\dots,N-1\end{cases} \tag{22}$$

$$B_i=\begin{cases}1-C_i, & i=1\\ 1-C_i-A_i, & i=2,\dots,N-1\\ 1-A_i, & i=N\end{cases} \tag{23}$$

In discretized form, Eq. (5) is

$$\left(\rho c_{j-1}\frac{\Delta x_{j-1}}{2}+\rho c_j\frac{\Delta x_j}{2}\right)\frac{T_j^{n+1}-T_j^n}{\Delta t}$$
$$=\frac{k_{j-1}}{\Delta x_{j-1}}\left(T_{j-1}^n-T_j^n\right)-\frac{k_j}{\Delta x_j}\left(T_j^n-T_{j+1}^n\right)$$
$$+\frac{1}{3\beta_{j-1}\Delta x_{j-1}}\left(G_{j-1}^n-G_j^n\right)-\frac{1}{3\beta_j\Delta x_j}\left(G_j^n-G_{j+1}^n\right) \quad (24)$$

where superscripts have been added to T and G to indicate the time step. Solving for T_j^{n+1} gives

$$T_j^{n+1}=T_j^n-\frac{2\Delta t}{\rho c_{j-1}\Delta x_{j-1}+\rho c_j\Delta x_j}\left[\frac{k_j}{\Delta x_j}\left(T_j^n-T_{j+1}^n\right)\right.$$
$$+\frac{1}{3\beta_j\Delta x_j}\left(G_j^n-G_{j+1}^n\right)+-\frac{k_{j-1}}{\Delta x_{j-1}}\left(T_{j-1}^n-T_j^n\right)$$
$$\left.-\frac{1}{3\beta_{j-1}\Delta x_{j-1}}\left(G_{j-1}^n-G_j^n\right)\right] \quad (25)$$

The material properties of the metallic foam, ρc, k, and β are all functions of temperature given by either polynomial approximations or interpolated from tabulated data. The temperature used for $\zeta_i=\rho_i c_i$, k_i, or β_i is the average temperature of the two endpoints of the interval Δx_i. Explicitly, for $\zeta=\zeta(T)$,

$$\zeta_i=\zeta[(T_i+T_{i+1})/2] \quad (26)$$

IV. Simulated Experiments

In this section, the simulated experiment for determining the thermal properties of the metallic foam is described. The simulated experiment consists of heating the (one-dimensional) sample of nickel foam at some pressure, for a particular time period, with a heater of a specified power, while taking temperature measurements at one location in the body (Fig. 1). Thus, the variables of the experiment are the heater power, the sensor location, the pressure, the heating time, and the total duration of the experiment.

Increasing the power to the heater increased the ability to determine the material properties. Because there would be physical limitations on the heater power supplied, rather than using the power of the heater as a variable between different experiments, an approximation of a heating apparatus used by Daryabeigi et al.[16] was made. This apparatus consisted of 2500-W cylindrical heating elements spaced 1.27 cm apart. This corresponds to about 93235 W/m^2 and an effective thickness of $b=0.005$ m. The effective thickness was determined by finding the thickness of a rectangle with width 1.27 cm with the same cross-sectional area as the data specifications of a Philips 2500T3/CL quartz lamp. The flux used was also specified by the manufacturer. The heater and the sample were placed 5.08 cm apart. A cold plate, kept at room temperature (300.6 K), is considered to be along the other side of the sample. For all of the examples, the thickness of nickel foam was 13.6 mm.

The temperature of the heater is determined from a lumped mass model. Under this model, the heater must satisfy the differential equation

$$\rho_h c_h b\frac{\partial T_h}{\partial t}=q_{\text{in}}-q_{\text{out}} \quad (27)$$

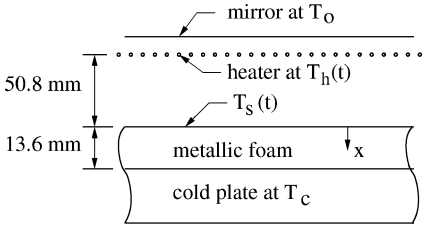

Fig. 1 Simulated experiment geometry.

where $\rho_h=2650$ kg/m^3 is the density of the heater and $c_h=745$ J/(kg · K) is the specific heat of the heater.[14] The power supplied to the heater is $q_{\text{in}}=93235$ W/m^2 when the heater is fully powered and zero otherwise. Here, q_{out} is the heat loss to the sample and the surroundings.

The losses from the heater include radiative transfer to the surroundings and to the sample. The radiative heat losses are given by

$$q_{\text{out}}^r=\epsilon_h\sigma\left(T_h^4-T_0^4\right)+\epsilon_1\sigma\left(T_h^4-T_s^4\right) \quad (28)$$

where $\epsilon_h=0.17$ is the emittance of a water-cooled mirrored surface (stainless steel[14]) behind the heater and T_0 is 300.6 K. Gas conduction from the heater to the sample is also included, described by

$$q_{\text{out}}^c=k_g\frac{\partial T}{\partial x} \quad (29)$$

The total heat flow out of the heater is $q_{\text{out}}=q_{\text{out}}^r+q_{\text{out}}^c$.

At each time step, the new surface temperature, node 1 in the discretized form of the heat equation, is determined through an energy balance. The heat flux into the surface consists of the radiative flux from the heater to the sample, the second term in Eq. (28), and the gas-conduction heat flux from the heater, Eq. (29). The heat flowing out of the surface is found by applying forward differences to Eqs. (2) and (4).

A typical experiment starts at room temperature, then the heater is powered for a period of time while the temperature is sampled at a particular location. Sampling continues for an additional period after the heater power is off. The heater model is incorporated into the transient finite difference code after the temperatures for each time step are found. There were 40 equally spaced divisions used across the 13.6-mm sample, resulting in a step size of 0.34 mm. A time step of 1 ms was used. Decreasing the time step by a factor of 10 changed the surface temperature during the experiment by at most 0.0008%, whereas increasing the step size by a factor of 10 resulted in a 0.01% increase in the surface temperature.

V. Optimality Criterion

The goal of this study is to examine a wide range of simulated experiments and determine the best experiment for determining the properties of the metallic foam. The suitability of individual experiments is determined from the sensitivity of the temperature with respect to the sought-after thermal properties of the sample, F, a, e_0, e_1, and ω. Relabeling the parameters b_k, $k=1,\ldots,p$, the normalized sensitivity coefficient for the kth parameter at the ith time step is defined as

$$X_k(i)=b_k\frac{\partial T_i}{\partial b_k} \quad (30)$$

Perturbing the parameters by a small amount, $(1+\delta)b_k$, the sensitivity coefficients can be approximated by

$$X_k(i)\approx\{T_i[(1+\delta)b_k]-T_i(b_k)\}/\delta, \qquad k=1,\ldots,p \quad (31)$$

The value of $\delta=0.0001$ was found to give well-behaved values for X.

In general, an experiment is better if the sensitivity coefficients are larger. In addition, for experiments with more than one parameter the sensitivity coefficients must be linearly independent. For these reasons, the dimensionless optimality criterion used was

$$D=\frac{|\boldsymbol{X}^T\boldsymbol{X}|}{\left(nT_{\max}^2\right)^p} \quad (32)$$

The sensitivity matrix $\boldsymbol{X}$ of size $(n\times p)$ is defined by

$$\boldsymbol{X}^T=\left[b_1\frac{\partial\boldsymbol{T}}{\partial b_1},b_2\frac{\partial\boldsymbol{T}}{\partial b_2},\ldots,b_p\frac{\partial\boldsymbol{T}}{\partial b_p}\right] \quad (33)$$

Table 1 Parameter values for simulated experiments

Parameter	Value
e_0, m^2/kg	9.85
e_1, m^2/kg K	$-2.63E-03$
ω	$9.93E-01$
F	$6.85E-03$
a, (m K/W)^3	$3.89E+02$

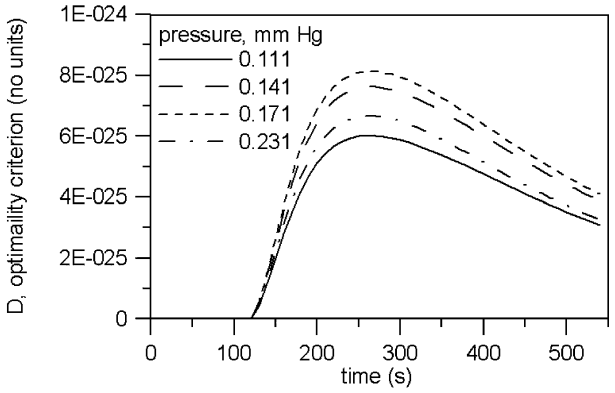

Fig. 2 D **with heating to** T_s **= 1273 K at various pressures in mm Hg.**

where $\boldsymbol{T}$ is a vector of the temperatures over all sampling times. Optimality criterion D is constructed from matrix $\boldsymbol{X}^T\boldsymbol{X}$, of size $(p \times p)$. Each element of matrix $\boldsymbol{X}^T\boldsymbol{X}$ has units $(\mathrm{K})^2$, and the determinant of $\boldsymbol{X}^T\boldsymbol{X}$, a scalar, has units $(\mathrm{K})^{2p}$. Therefore, in Eq. (32), D is normalized by the maximum temperature squared $T^2_{\max}$ and the number of sample temperatures n, all taken to the power p to obtain a fair comparison among different experiments.[3]

The sensitivities are partial derivatives at a particular value of each parameter. The parameter values used for this study are given in Table 1, as reported by Sullins and Daryabeigi.[12]

VI. Optimal Experiment Design

Our experience with thermal conductivity measurements, with no radiation present, suggested that it is best to heat the sample as rapidly as possible for a period of time while taking measurements at the surface closest to the heater. This is also the best approach for radiation/conduction materials. A variety of simulated experiments were explored by varying the pressure, the duration of the heating, and the total duration of the experiment. For experiments at lower pressures radiative heat transfer is more dominant, whereas at higher pressures heat transfer due to conduction is more significant. It was, thus, expected that the optimum case would occur at moderate pressures because three of the parameters are related to radiation, and two are related to conduction.

The approximate conditions for the optimum experiment were found first by trial and error to find a rough value of the maximum of D, after which an optimization routine was run with the rough value as the initial guess. The maximum temperature of interest and the maximum temperature at which the various material properties were valid was 1000°C (1273 K). For all of the experiments considered, it was found that, at a given pressure, D was maximized if the heater was operated until the surface of the metal foam reached $T_s = 1273$ K, and then data sampling was continued as the metal foam cooled. This effectively removed the heating time as a variable between experiments. The maximum value of D, subject to the temperature constraint, was $8.13E-25$. This value resulted from an experiment conducted at 0.171 mm Hg, in which the heater was run for 122 s and the temperature was sampled every 10 s for a total duration of 270 s. Heating the sample longer would have resulted in larger D values, but the surface of the metal foam would have exceeded the maximum allowable temperature of $T_s = 1273$ K.

In Fig. 2, the optimality criterion is graphed vs time for a few simulated experiments in which the pressure was varied around the optimal pressure and for which the sample is heated until the heater reaches 1273 K. The time before the sample reaches 1273 K is dependent on the pressure, and so the times vary slightly from 122 s. In Fig. 3, D is graphed vs time with the pressure fixed at 0.171 mm Hg for various heating times. In general, if the sample is continuously heated the D value rises to a maximum and then begins to decrease as the system reaches steady state. If instead the heater is shut off, at some time, the value of D dramatically increases until the system again nears steady state (room temperature). The rise in the D values when the heater is shut off is so dramatic that it is difficult to see unless a very small portion of the D curves are examined. In Fig. 4, the same curves given in Fig. 3 are repeated along with a curve corresponding to continuous heating. The small vertical scale in Fig. 4 shows the dramatic rise in the D values when the heater is turned off, compared to continuous heating. The continuous-heating curve, shown only for reference, does not represent a useful experiment because it would result in sample-surface temperatures in excess of 1273 K. In Table 2, the maximum values of D obtained for various pressures and heating times are listed.

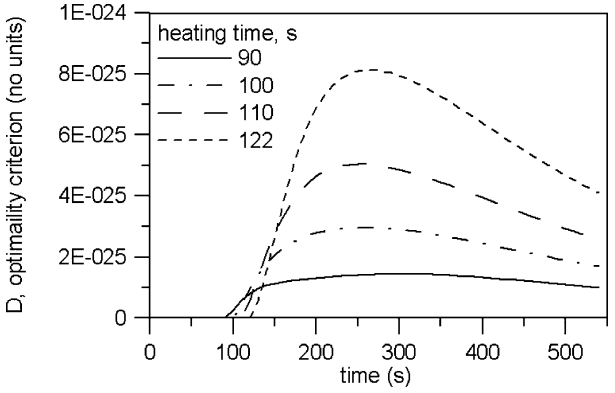

Fig. 3 D **for** P **= 0.171 mm Hg and various heating times.**

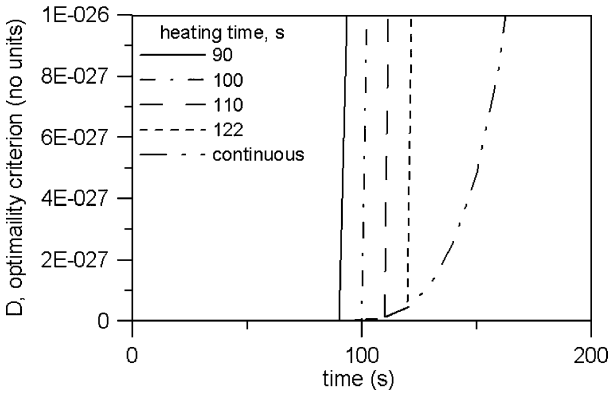

Fig. 4 D **for** P **= 0.171 mm Hg during heating.**

Note that for the optimal experiment one would want to stop taking data as soon as D reached its maximum value. From Fig. 2 or Fig. 3, this is at 270 s at pressure 0.171 mm Hg. This time is not too critical because for any value between 250 s and 280 s, D will still be within 0.5% of its maximum value at this pressure. Thus, for this model, the optimal experiment for determining the material properties is for the sample to be heated for 122 s at a pressure of 0.171 mm Hg with sampling every 10 s until 270 s have elapsed.

In Fig. 5, the heat flux for the optimal experiment is given as a function of time. Although conduction flux is larger soon after heating begins, and radiation flux is larger as the sample gets hotter, at all times both conduction and radiation are important, as expected. The temperature profile for the optimal experiment is given in Fig. 6. Note from the temperature profile that the system has not reached steady state when the heater is shut off at 122 s, nor at the optimal temperature-sampling duration of 270 s. The heater had to be shut off before the system was at steady state due to the temperature constraint on the sample.

Table 2 Maximum D values for experiments

	Heating duration, s					
P [mmHg]	95	100	105	110	115	122
0.071	$7.93E-26$	$1.10E-25$	$1.45E-25$	$1.80E-25$	$2.25E-25$	$2.70E-25$
0.121	$1.84E-25$	$2.57E-25$	$3.43E-25$	$4.28E-25$	$5.41E-25$	$6.67E-25$
0.171	$2.11E-25$	$2.97E-25$	$4.00E-25$	$5.04E-25$	$6.42E-25$	$8.13E-25$
0.221	$1.74E-25$	$2.48E-25$	$3.37E-25$	$4.29E-25$	$5.50E-25$	$7.15E-25$
0.271	$41.17E-25$	$1.70E-25$	$2.34E-25$	$3.00E-25$	$3.88E-25$	$5.18E-25$

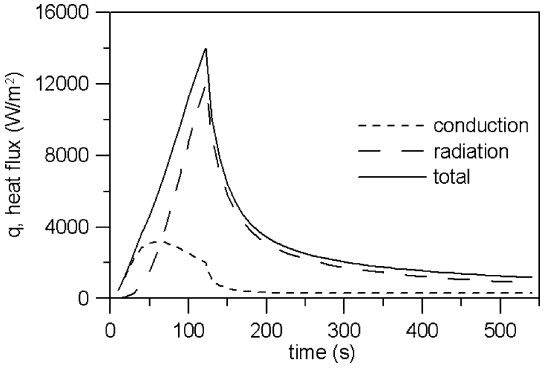

Fig. 5 Heat fluxes for $P = 0.171$ mm Hg and 122 s of heating.

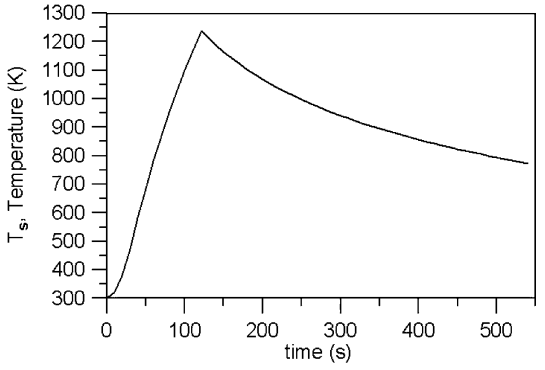

Fig. 6 Temperature for $P = 0.171$ mm Hg and 122 s of heating.

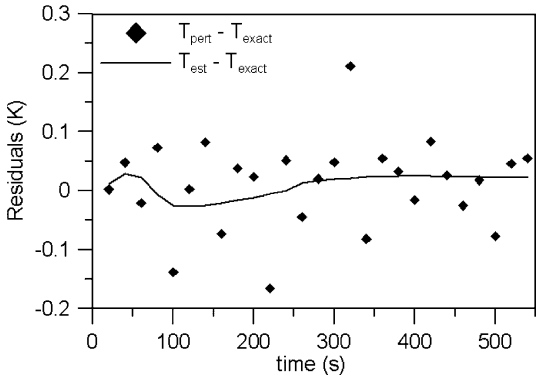

Fig. 7 Temperature residuals for simulated experiment 1.

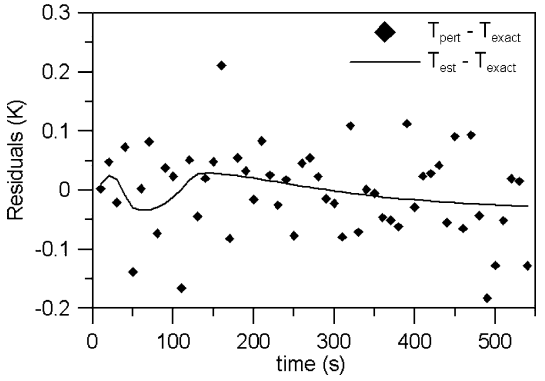

Fig. 8 Temperature residuals for simulated experiment 2.

VII. Estimation of Parameters

In this section, the parameters are determined using three simulated experiments. Experiment 1 is the experiment found using the optimality criterion in the preceding section. Experiment 2 is the same as experiment 1 except that data are taken for 540 s. Experiment 3 consists of two heating events concatenated into one simulated experiment, where one of the heating events is dominated by conduction flux and the other is dominated by radiative flux. Data for all of the simulated experiments are obtained by calculating the exact surface temperatures using the values of the parameters given in Table 1 and then corrupting them with random noise with a standard deviation of 0.08 K. The standard deviation was chosen to correspond with the maximum standard deviations reported by Sullins and Daryabeigi[12] for actual experiments in the same temperature range. A nonlinear Levenberg–Marquardt parameter estimation routine is used to fit the model parameters (see Ref. 17).

For simulated experiment 1, the optimum experiment determined in the preceding section was used. It consists of running the heater for 122 s and taking measurements until 270 s elapsed. The gas pressure is 0.171 mm Hg. The residuals between the exact and perturbed (noise added) temperatures, $T_{\text{pert}} - T_{\text{exact}}$, and between the exact temperatures and those calculated using the estimated parameters, $T_{\text{est}} - T_{\text{exact}}$, are given in Fig. 7. The residuals between the exact temperatures and those calculated with the estimated parameters are less than 0.03 K and are biased toward overestimating the exact temperatures. The estimated values of the parameters along with their 90% confidence intervals are given in Table 3. The parameter estimates for F and a have errors over 1%.

Because at 270 s the temperature was still significantly above room temperature, for simulated experiment 2 the same heating time of 122 s was used, but the temperature sampling was extended to 540 s. By 540 s, the temperature at the sensor had cooled to 774 K. The results of parameter estimation for experiment 2 were slightly worse in terms of the residuals with a maximum error of 0.034 K (solid line, Fig. 8) compared to a maximum error of 0.029 K for experiment 1 (solid line, Fig. 7). The parameter estimates for F and a improved in experiment 2, but the estimates for the radiation related parameters were considerably worse (Table 4). This is probably because conduction flux becomes more important as the sample cools (Fig. 5). Further extensions of the experiment duration, beyond 540 s, were found to give the same effect as experiment 2.

Various other experiments to find all of the parameters accurately with a single heating event were tried without success. At high pressures, the flux due to conduction is dominant, whereas at low pressures the radiation flux is dominant. Therefore, a and F will be more important in experiments conducted at high pressure. Conversely, e_0, e_1, and ω should be more important and, hence, determined with more precision when the pressure is low. Based on this information, simulated experiment 3 was constructed from a pair of heating events: one at high pressure and one at low pressure. Noise was added to the data from this pair of heating events. The

Table 3 Parameter values for simulated experiment 1

Parameter	e_0	e_1	ω	F	a
Exact	9.850+00	−2.630E−03	9.930E−01	6.850E−03	3.890+02
Estimated	9.848+00	−2.623E−03	9.930E−01	6.955E−03	3.523+02
Percent Error	−1.771E−02	−2.681E−01	−3.884E−03	1.529E00	−9.429E00
90% confidence interval	1.752E−01	1.817E−04	1.652E−04	5.894E−04	1.870+02

Table 4 Parameter values for simulated experiment 2

Parameter	e_0	e_1	ω	F	a
Exact	9.850+00	−2.630E−03	9.930E−01	6.850E−03	3.890+02
Estimated	9.800+00	−2.571E−03	9.929E−01	6.912E−03	3.657+02
Percent error	−5.100E−01	−2.245E+00	−5.408E−03	9.030E−01	−5.993E+00
90% confidence interval	1.076E−01	1.081E−04	1.572E−04	5.694E−04	1.852+02

Table 5 Parameter values for combined conduction and radiation experiments

Parameter	e_0	e_1	ω	F	a
Exact	9.850+00	−2.630E−03	9.930E−01	6.850E−03	3.890+02
Estimated	9.864+00	−2.644E−03	9.930E−01	6.862E−03	3.876+02
Percent error	1.371E−01	5.348E−01	3.161E−03	1.683E−01	−3.572E−01
90% confidence interval	1.104E−01	1.189E−04	8.444E−05	2.440E−05	2.737+00

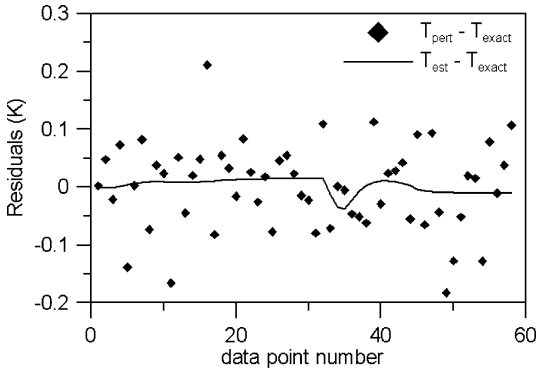

Fig. 9 Temperature residuals for simulated experiment 3.

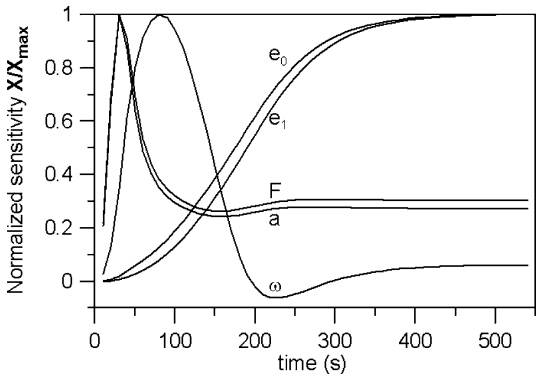

Fig. 10 Sensitivities for simulated experiment 2.

data sets were then concatenated as one data set for the parameter estimation.

Increasing the experiment pressure was found to improve the estimation of a and F. However, an increase in pressure from 1 to 10 atm increased the D values (for F and a) by only 0.03%. Because it would be much easier to obtain a pressure of 1 atm, this was used for the conduction-optimum (high-pressure) heating event. In this case, it was also found that using more power in the heater was better and that it was best to heat the sample until it reaches 1273 K. Therefore, the only variable to determine was how long to sample the temperature. At 1 atm, the sample reached 1273 K in 133 s and D reached a maximum at 320 s. Although this heating event was primarily to determine a and F, all five parameters were considered variables in determining D because they all would be unknown when the data were analyzed.

For the radiation-optimal (low-pressure) heating event, radiative heat transfer is the largest for a vacuum (no gas conduction). Sullins and Daryabeigi[12] reported using a minimum pressure of 0.0001 mm Hg, and so this value was chosen as a practically obtainable minimum pressure. Again it was found that it was best to heat the sample using the maximum amount of power until the sample reached 1273 K. The sample reached 1273 K after 121 s of heating and D was at a maximum at 260 s.

Simulated experiment 3 consisted of the conduction-optimal and radiation-optimal heating events combined together. The residuals for simulated experiment 3 are given in Fig. 9. In Fig. 9, the first 32 data points shown are from the conduction-optimal heating event, and the last 26 points are from the radiation-optimal heating event. The estimated parameters and their 90% confidence intervals are given in Table 5. As can be seen in Fig. 9 and Table 5, the temperatures and the parameters are estimated accurately.

The sensitivity coefficients (normalized by their maximum value) are plotted for simulated experiment 2 in Fig. 10. The sensitivity for a has nearly the same shape as the sensitivity for F. This indicates that the sensitivities are almost linearly dependent, and this is probably the reason that it is hard to determine the value for a. A different choice of conduction parameters could probably be found that could be determined more accurately from simulated or actual experiments. Simulated experiment 3 provides more accurate results than either experiment 1 or 2. Using two heating events reduced the dependency of the sensitivities of F and a.

VIII. Conclusions

For the future use of high-porosity materials in thermal protection systems for reusable launch vehicles, their performance needs to be characterized over a wide range of temperatures and pressures. The goal of this research is to develop general-purpose protocols for designing transient experiments to measure thermal properties of high-porosity materials. As a first step, a metal-foam material was studied with an experimentally validated thermal model.

The D optimality criterion and consideration of the heat fluxes can lead to suitable experiments for determining the properties.

Maximization of the optimality criterion D provides an experiment containing one heating event that could be used to determine the radiation and conduction parameters. Extending the duration of the experiment did not improve the parameter estimation. By consideration of the model itself and, in particular, its conduction and radiation behavior, a set of two heating events were found that, considered together, provided the most accurate parameter estimates.

The radiation parameter ω was easily found to a high degree of accuracy by all of the experiments. The coupling coefficient a was the hardest parameter to determine. The sensitivity of the coupling coefficient and the sensitivity of the solid conduction efficiency F are similar in shape, which indicates that they are close to linearly dependent. The coupling coefficient was an ad hoc parameter added to the model of Sullins and Daryabeigi[12] to obtain agreement with experimental data at high pressures. This suggests that there may be a different pair of conduction parameters that could adequately model the conduction process and provide a more robust estimation than was exhibited here.

Acknowledgment

This work was supported by NASA Langley Research Center Grant NAG-1-01087, under the supervision of Max Blosser. The views expressed in this article are those of the authors and do not reflect the policy or position of the U.S. Air Force, Department of Defense, or the U.S. government.

Appendix: Temperature-Dependent Nitrogen Properties

The temperature-dependent properties for nitrogen are from Daryabeigi[13]:

$$\rho_g = -1.734E-4 + 342.216/T \tag{A1}$$

$$c_g = 1.083.545 - 0.328T + 6.949E-4T^2 - 2.82E-7T^3 \tag{A2}$$

$$k_g = 2.048E-3 + 8.751E-5T - 2.462E-8T^2 \tag{A3}$$

$$Pr = 0.854 - 7.085E-4T + 9.008E-7T^2 - 3.207E-10T^3 \tag{A4}$$

References

[1]Dorsey, J. T., Poteet, C. C., Wurster, K. E., and Chen, R. R., "Metallic Thermal Protection System Requirements, Environments, and Integrated Concepts," *Journal of Spacecraft and Rockets*, Vol. 41, No. 2, 2004, pp. 162–172.

[2]Beck, J. V., and Arnold, K. J., *Parameter Estimation*, Wiley, New York, 1977, pp. 400–413.

[3]Taktak, R., Beck, J. V., and Scott, E. P., "Optimal Experimental Design for Estimating Thermal Properties of Composite Materials," *International Journal of Heat and Mass Transfer*, Vol. 36, No. 12, 1993, pp. 2977–2986.

[4]Dowding, K. J., and Blackwell, B. F., "Sensitivity Analysis for Nonlinear Heat Conduction," *Journal Heat Transfer*, Vol. 123, No. 1, 2001, pp. 1–10.

[5]Cole, K. D., "Thermal Characterization of Functionally Graded Materials–Design of Optimal Experiments," *Journal of Thermophysics and Heat Transfer*, Vol. 18, No. 3, 2004, pp. 289–294.

[6]Cole, K. D., "Analysis of Photothermal Characterization of Layered Materials: Design of Optimal Experiments," *International Journal of Thermophysics*, Vol. 25, No. 5, 2004, pp. 1567–1584.

[7]Yuen, W. W., Takara, E., and Cunnington, G., "Combined Conductive/Radiative Heat Transfer in High Porosity Fibrous Insulation Materials: Theory and Experiment," Paper TED-AJ03-126, March 6th American Society of Mechanical Engineers–Japan Society of Mechanical Engineers, Tokyo, Joint Thermal Engineering Conf., 2003.

[8]Daryabeigi, K., "Heat Transfer in High-Temperature Fibrous Insulation," *Journal of Thermophysics and Heat Transfer*, Vol. 17, No. 1, 2003, pp. 10–20.

[9]Boomsma, K., and Poulikakos, D., "On the Effective Thermal Conductivity of a Three-Dimensionally Structured Fluid-Saturated Metal Foam," *International Journal of Heat and Mass Transfer*, Vol. 44, No. 4, 2001, pp. 827–836.

[10]Bhattacharya, A., Calmidi, V. V., and Mahajan, R. L., "Themophysical Properties of High-Porosity Metal Foams," *International Journal of Heat and Mass Transfer*, Vol. 45, No. 5, 2002, pp. 1017–1031.

[11]Zhu, H., Sankar, B. V., Haftka, R. T., and Venkataraman, S., "Minimum Mass Design of Insulation Made of Functionally Graded Material," *Journal of Spacecraft and Rockets*, Vol. 41, No. 3, 2004, pp. 467–469.

[12]Sullins, A. D., and Daryabeigi, K., "Effective Thermal Conductivity of High Porosity Open Cell Nickel Foam," AIAA Paper 2001-2819, June 2001.

[13]Daryabeigi, K., "Design of High Temperature Multilayer Insulation for Reusable Launch Vehicles," Ph.D. Dissertation, Mechanical and Aerospace Engineering Dept., University of Virginia, Charlottesville, VA, May 2000.

[14]Incropera, F. P., and De Witt, D. P., *Introduction to Heat Transfer*, 2nd ed., Wiley, New York, 1990, pp. A8–A25.

[15]Rohsenow, W. M., Hartnett, J. P., and Cho, Y. I., *Handbook of Heat Transfer*, McGraw–Hill, New York, 1973, Chap. 2, p. 107.

[16]Daryabeigi, K., Knutson, J. R., and Sikora, J. G., "Thermal Vacuum Facility for Testing Thermal Protection Systems," NASA TM-2002-211734, June 2002.

[17]Press, W. H., Flannery, B. P., Teukolsky, S. A., and Vetterling, W. T., *Numerical Recipes in FORTRAN 77*, Cambridge Univ. Press, New York, 1989, pp. 523–528.